PHYSICAL REVIEW B VOLUME 58, NUMBER 4 15 JULY 1998-II

Surface morphologies in GaAs homoepitaxy: Mound formation and evolution

V. R. Coluci, M. A. Cotta, C. A. C. Mendonça, K. M. I.-Landers,
and M. M. G. de Carvalho
Universidade Estadual de Campinas, Instituto de Física Gleb Wataghin, Departamento de Física Aplicada/Laboratório de Pesquisa em Dispositivos, Caixa Postal 6165, 13081-970, Campinas, São Paulo, Brazil
(Received 10 July 1997; revised manuscript received 16 January 1998)

Atomic force microscopy has been used to observe surface morphologies during growth of GaAs films on GaAs(001) by chemical beam epitaxy. Mound formation is observed at the beginning of GaAs growth as a function of the surface prior to deposition. GaAs substrates exhibit a large density of pits and cracks after usual thermal treatment employed for oxide desorption. On this kind of surface mounds form and coalesce as film thickness increases; surface planarization is eventually achieved—at this point, morphologies are typically those expected from two-dimensional growth. In this sense we observe that monolayer island size distribution is determined by the kinetic conditions used for the growth; nucleation sites and island spatial distribution, however, are strongly influenced by the topography of the initial surface where the film is deposited even for films thousands of monolayers thick. The final morphologies present wide terraces and few monolayer islands on top of them independent of growth conditions. This picture agrees with theoretical results where negligible step edge barriers are considered. [S0163-1829(98)02328-5]

Interfaces in semiconductor heterostructures constitute an important issue today, either for basic knowledge or for applications in the design of new structures or devices. In particular, interfaces grown by molecular beam epitaxy (MBE) and related techniques have been widely studied in order to achieve a detailed understanding of surface morphology and its time evolution. Such studies can provide fundamental information on the underlying kinetic phenomena and the resulting growth modes.

It has been shown that these growth processes can give rise to a wide variety of surface morphologies, even when simple homoepitaxy is considered. Generally, models describing MBE growth present stable layer-by-layer growth mode or kinetically rough films resulting from multilayer growth at low temperatures. Recently, however, unstable three-dimensional growth that can result in pyramidlike features—or mounds—has been predicted by continuum models.[1,2] These structures were then observed in computer simulations using the solid-on-solid model[3,4] and experimentally in several systems as GaAs/GaAs(001),[5–8] Cu/Cu(001),[9,10] Ge/Ge(001),[11] and Fe/Fe(001).[12] This unstable growth mode is associated with the existence of energy barriers near step edges that inhibits interlayer diffusion[13] and creates a diffusion bias on the growing surface.[14] The instability occurs for singular surfaces since mounds are only present when there is sufficient nucleation of islands on terraces—when the slope of the surface is small enough. Vicinal surfaces with miscut above a certain value are stable. Mound sizes have been shown to increase during growth through a coarsening process;[7,15] the mound slope, on the other hand, has been observed to grow in some experiments[11,16] and to remain approximately constant in others.[6,7,9,12] In the particular case of GaAs homoepitaxial films grown by MBE, Orme *et al.*[7,15] have shown that multilayered features evolve on the surface when growth conditions favor island nucleation. As the epilayer thickness is increased these mounds grow in all dimensions with the slope remaining approximately constant at 1°. In another work, Van Nostrand *et al.*[8] extensively characterized the surface roughness of 500-nm-thick GaAs(001) layers grown by MBE and gas source MBE. They observed a surface morphology consisting of a regular array of multilayer growth mounds sensitive to growth temperature in both cases. In the particular case of gas source MBE, mounds were observed for GaAs films grown at 500 and 585 °C directly on the substrates (with no GaAs buffer layer); mounds grown at 585 °C present sizes at least twice as large as those grown at 500 °C. In this work, the authors also suggest an effect of hydrogen on mound shape since MBE-grown samples present more elongated mounds than gas source MBE samples.

In this paper we present a study on the nucleation of GaAs homoepitaxial films by chemical beam epitaxy (CBE). We discuss mound formation and the role of the starting surface for deposition. We show that monolayer island size distribution is determined by the kinetic conditions employed for the growth; the nucleation sites and spatial distribution, however, are related to the topography of the initial surface where the film is deposited even for thicknesses of thousands of monolayers. Mound formation is observed only when a large density of pits is present on the initial surface and is associated to a stage in the healing process of this surface: For thick films, the final morphologies present wide terraces and few monolayer islands on top of them, independent of growth conditions. These results and the absence of mounds for films grown on initially flat surfaces suggest a negligible step edge barrier for GaAs grown by CBE.

The samples used in this study were grown by CBE using triethylgallium (TEG) diluted with hydrogen carrier gas as group III source and thermally decomposed pure arsine (AsH_3) as group V source. Mass spectrometry analysis indicates that the hydride is totally decomposed at the cracker cell temperature used here (1050 °C). Growth temperatures were in the range 510–550 °C measured by infrared pyrometers. This temperature range was chosen in order to keep the GaAs growth rate approximately constant, by assuring a fast

 © 1998 The American Physical Society

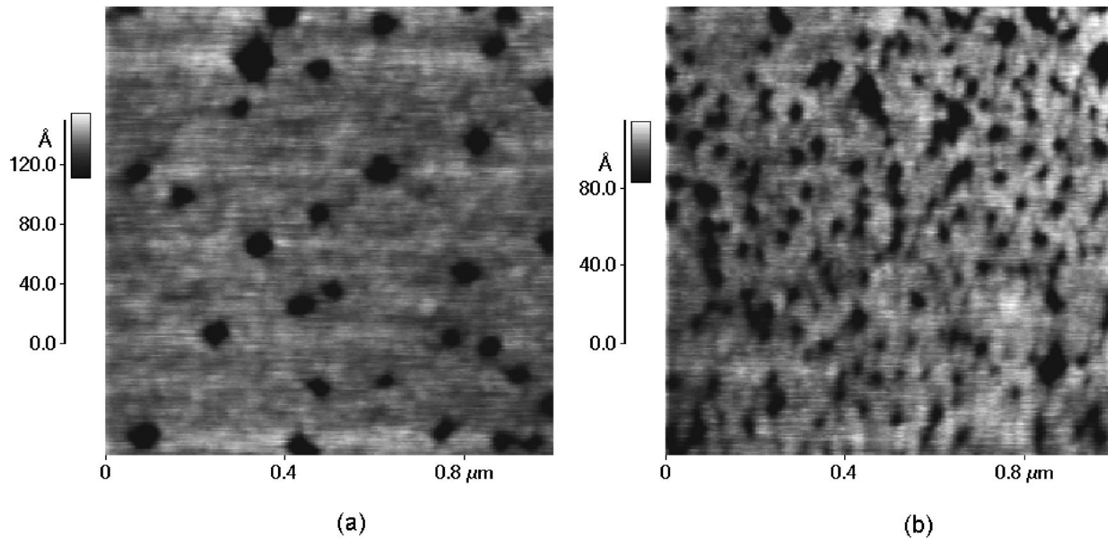

FIG. 1. AFM images of GaAs surfaces after thermal treatment for oxide desorption: (a) nominal and (b) 2° off substrate.

TEG decomposition on the GaAs surface and preventing the evaporation of Ga-related species from the growing surface.

The GaAs films were grown simultaneously on (001) GaAs substrates nominally oriented and 2° off towards the nearest ⟨110⟩ direction. The substrates were heated at 590 °C for 5 min under As_2 flow for oxide desorption and annealing of the surface. The GaAs films were then deposited either directly on the substrate or on the top of a 1500-nm-thick GaAs buffer layer. The film thicknesses were varied between 50 and 1500 nm. The growth rate was varied in the range

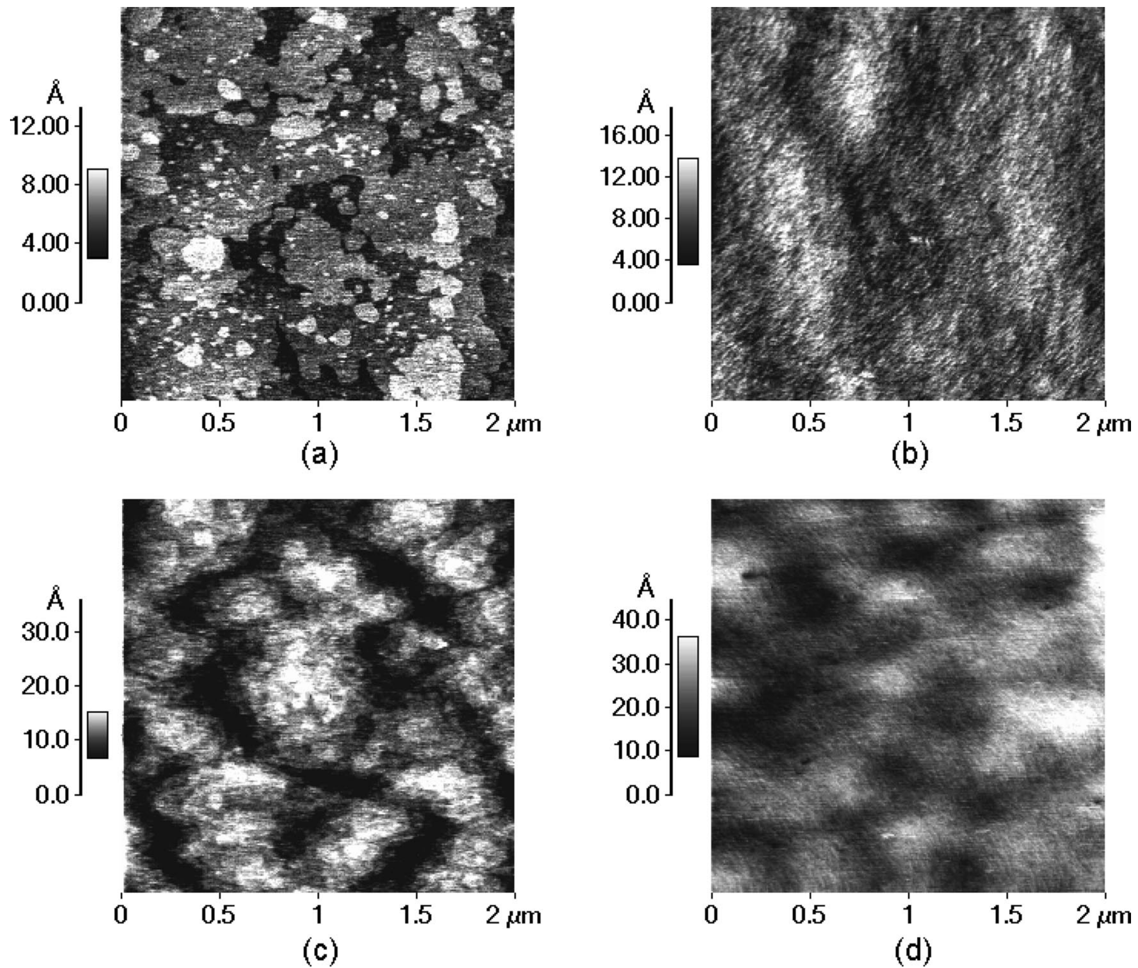

FIG. 2. AFM images of homoepitaxial GaAs films grown under the same conditions (550 °C, growth rate=0.4 nm/s) on nominal (a), (c) and 2° off substrates (b), (d). Samples shown in (a), (b) are 1500 nm thick and samples shown in (c), (d) are 300 nm thick.

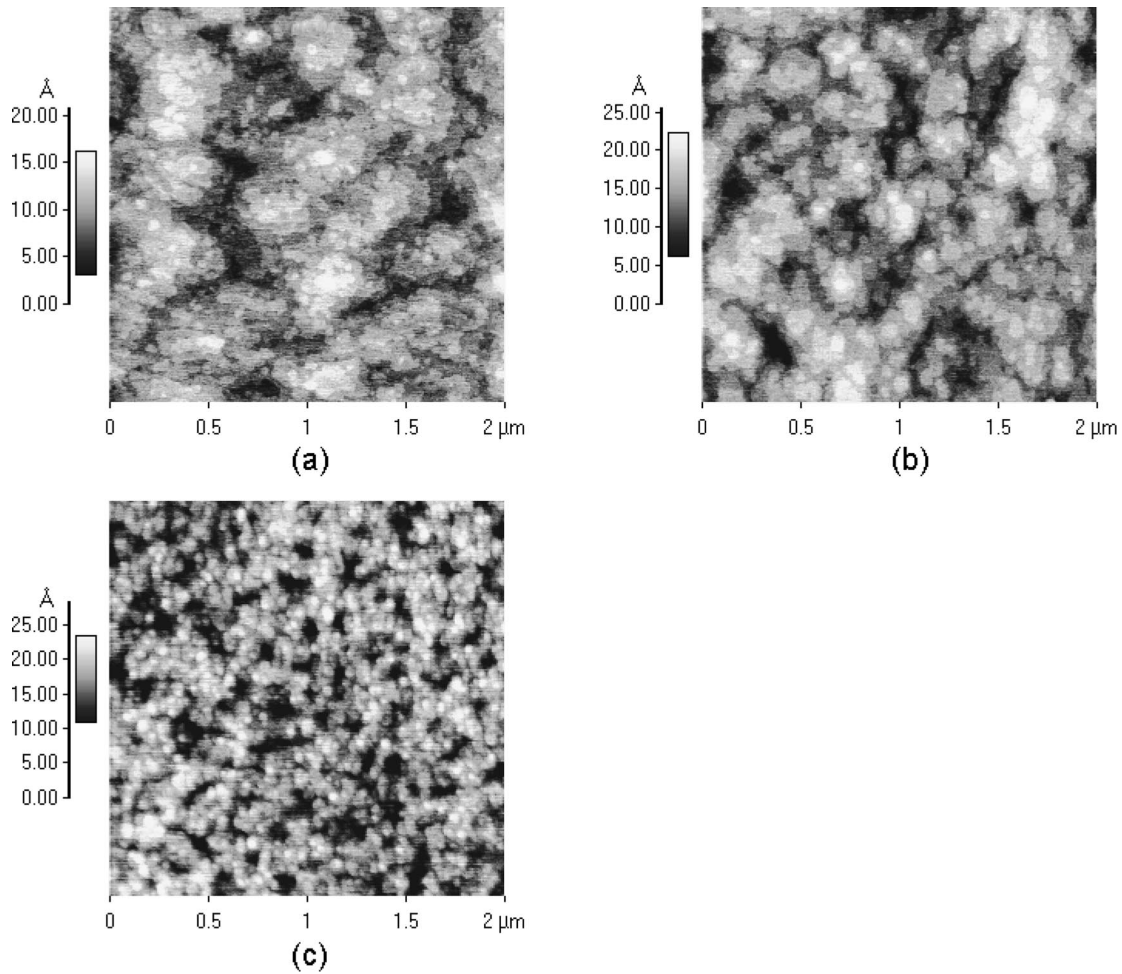

FIG. 3. AFM images of 300 nm thick homoepitaxial GaAs films grown by CBE using different TEG+H_2 flows with corresponding GaAs growth rates: (a) 0.2 nm/s, (b) 0.4 nm/s, and (c) 0.8 nm/s.

≈0.2–0.8 nm/s for different As_2 flows. The morphology of the films was observed by in-air atomic force microscopy after removal of the samples from the growth chamber and exposure to air.

Figure 1 shows the surface of the GaAs substrate after oxide removal and annealing. The surface topography is dominated by the presence of pits that have also been observed in MBE samples.[5–7] The pits are typically 40–60 nm in lateral size and 5–10 nm deep. No crystalline facets could be observed with the AFM; sidewall angles varied in the range 15–28°. A large density of pits is observed for both the 2°off (~140 μm^{-2}) and the nominal (~30 μm^{-2}) substrates. The morphology in between pits, however, is relatively smooth (rms roughness ~0.35 nm). In fact, high-energy electron diffraction from the annealed substrates shows typical two-dimensional patterns due to the relatively large distance between pits. The pits are not present in the as-loaded GaAs wafer, and the pit density values are much higher than those of crystalline defects expected in these substrates from double crystal x-ray diffraction and etch pit density measurements. On the other hand, the presence of pits does not depend on the substrate annealing time but on the surface characteristics prior to growth. Epiready substrates with the same overall characteristics but from different batches present different pit densities. This indicates that the pits are formed by an etching process induced at certain regions of the substrate and intrinsically related to the oxide-desorption process. Using multiple x-ray diffraction Morelhão *et al.*[17] showed that the polishing process commonly used in high-quality commercially available substrates is related to a larger misorientation of crystal blocks (with sizes up to hundreds of nanometers) near the surface, when compared to a deeply etched (up to ~10 μm deep) surface of the same substrate. These large crystal blocks may be related to pit formation due to a preferential etching of the material in the regions close to the block boundaries.

TABLE I. rms roughness (W) and peak-to-valley (P-V) height variation for samples shown in Fig. 3.

GaAs growth rate (nm/s)	W (Å)	P-V (Å)
0.2	2.6±0.4	23±4
0.4	3.2±0.3	26±4
0.8	3.2±0.2	30±4

The GaAs film morphology, as expected from a stable two-dimensional layer-by-layer growth mode can be observed in Figs. 2(a) and 2(b). The 1500-nm-thick film morphology presents wide monolayer terraces (height ~0.3 nm)

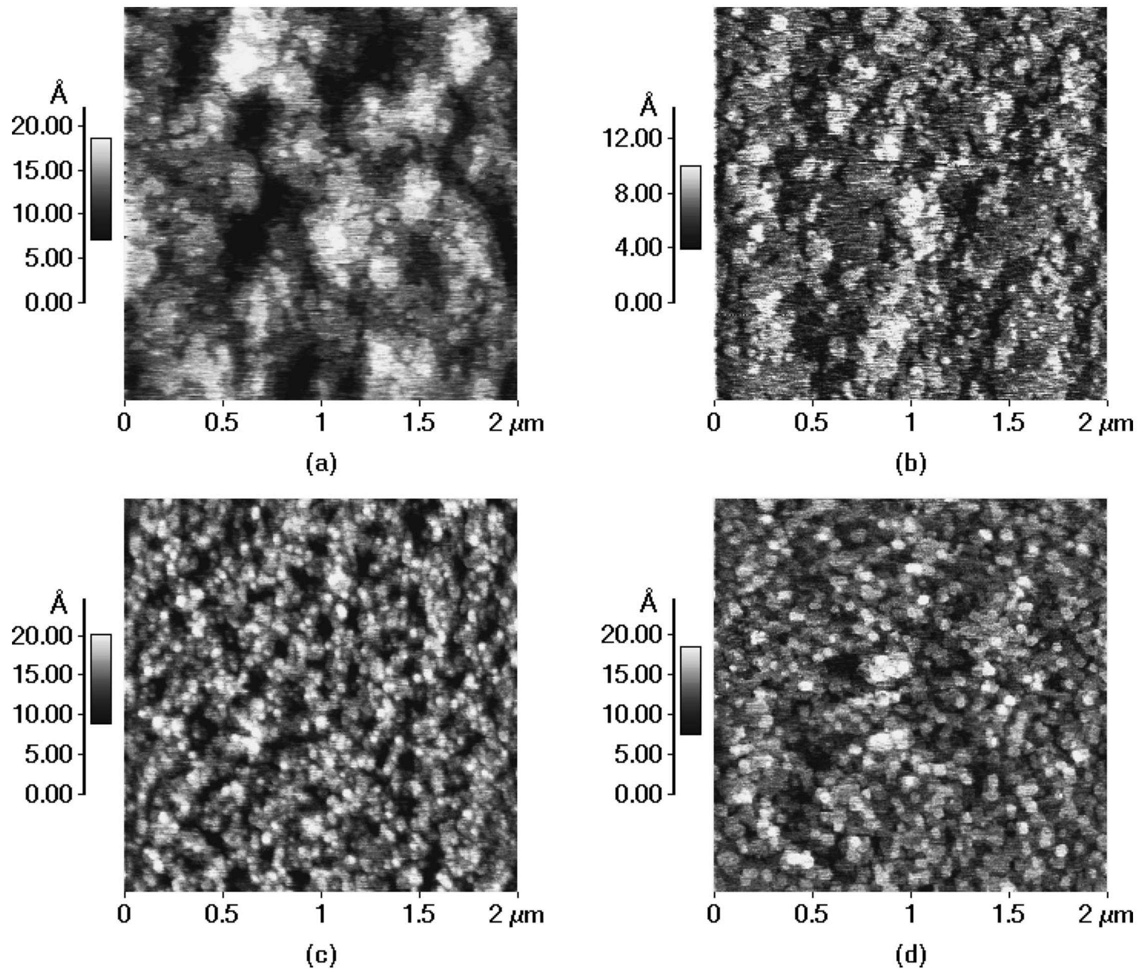

FIG. 4. AFM images of homoepitaxial GaAs films grown on (a), (c) substrate surface after thermal treatment for oxide desorption (cf. Fig. 1) and (b), (d) 1500-nm-thick GaAs buffer layer [cf. Fig. 2(a)]. All samples were grown at 530 °C with growth rates: (a), (b) 0.2 nm/s and (c), (d) 0.8 nm/s.

on nominal surfaces [Fig. 2(a)]. The same structure and height variation are observed for both nominal and 2° off substrates, although terrace widths in the 2° off case are below the AFM lateral resolution.

When film thickness is reduced to 300 nm, under the same growth conditions [Figs. 2(c) and 2(d)], we can observe a larger height variation in the AFM image, as well as the formation of almost circular features on the surface [Fig. 2(c)], similar to those observed by Van Nostrand *et al.*[8] for gas source MBE samples. These features are formed by the simultaneous nucleation of several monolayers, forming much narrower terraces than in the case of thicker films. Again for the 2° off substrates the terrace structure is not observable but the height variation profile along the surface suggests that the same features form on these samples.

At lower growth temperatures, this effect is more noticeable, as shown in Fig. 3. Here the morphologies of 300-nm-thick GaAs films grown on nominal substrates at 530 °C with different TEG flows are imaged with the AFM. For the same film thickness (300 nm), we can observe that similar morphologies are observed at 550 [Fig. 2(c)] and 530 °C [Fig. 3(a)]. For this particular set of samples, a smaller TEG flow was used at the lower temperature, indicating that the final morphology at a certain thickness is kinetically controlled. Indeed, at 510 °C mounds are present even for much thicker films. Figure 3 also shows that at constant temperature the size of the circular features decrease as the TEG flow is increased. Slightly larger values of rms roughness and peak-to-valley height variation are associated to the samples grown with larger growth rate (Table I), but they are still similar to those observed for typical GaAs morphologies [Figs. 2(a) and 2(b)]. The change in morphology when mounds are present is accomplished by the coalescence—and the resulting increase in size—of the incomplete terraces at the bottom of the structures. This picture corresponds to a healing process of the initial surface, filling up the pits observed in Fig. 1. The pits correspond to cracks in the singular surface of the crystal; the deposition of the GaAs epitaxial film is then slowly healing these cracks. For thicker films [Figs. 2(a) and 2(b)] the morphology shows no signs of the earlier presence of irregularities.

The circular features resemble closely the mounds predicted by several models to be formed on nominal surfaces when a diffusion bias is considered for adatom hopping on the surface.[4,18] Our results, however, point to a different origin for such features in our samples. Figure 4 shows the morphologies of 300-nm-thick GaAs films grown on different surfaces for two sets of growth conditions. For samples shown in Figs. 4(a) and 4(c) the film was grown directly on a nominal substrate after oxide desorption and annealing as

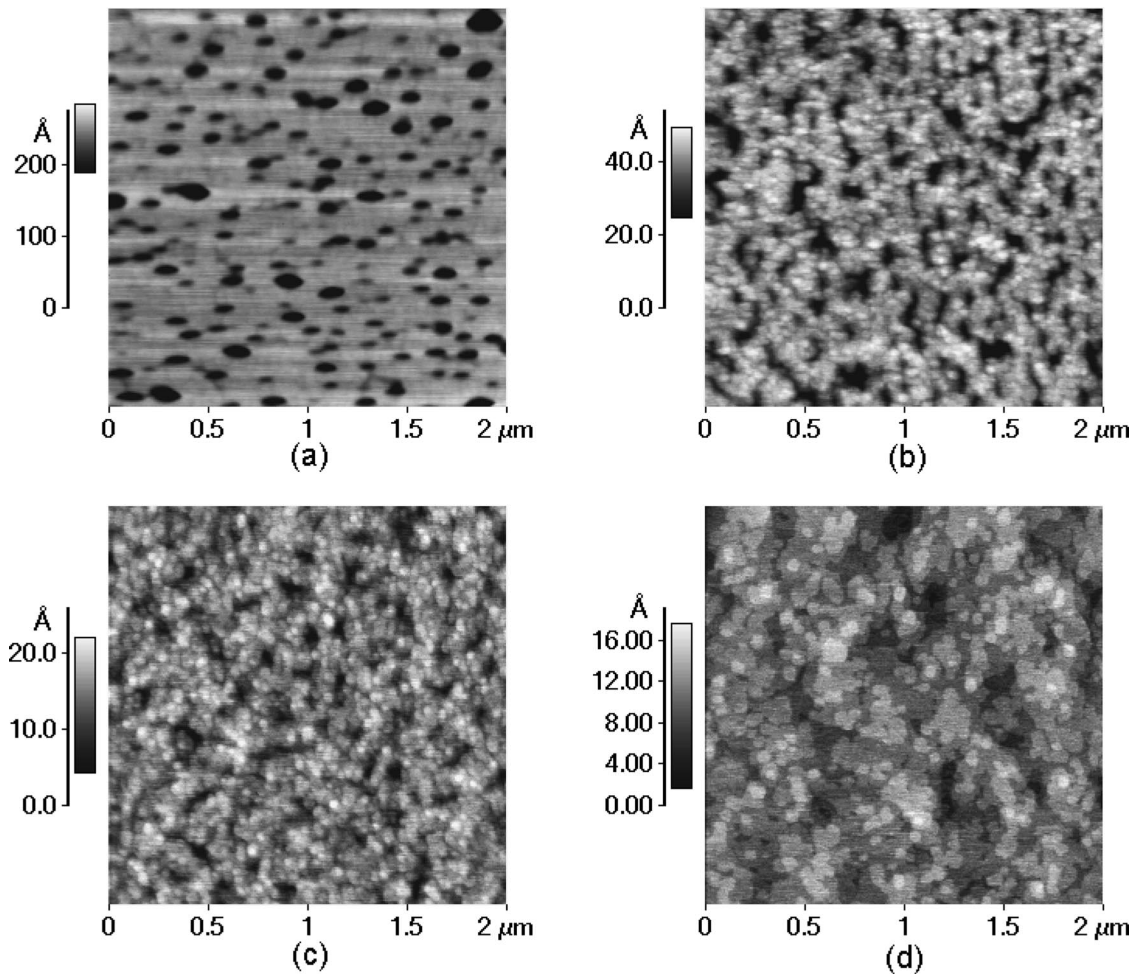

FIG. 5. AFM images of GaAs films grown under the same conditions (530 °C, growth rate=0.8 nm/s) and different thicknesses: (a) 50 nm, (b) 150 nm, (c) 300 nm, and (d) 1500 nm.

described above. Figures 4(b) and 4(d) present the morphologies of the GaAs films grown on top of a 1500-nm-thick GaAs buffer layer, with morphology similar to that shown in Fig. 2(a). The circular features—or mounds—are not present in this case. The average size of the islands observed in Figs. 4(a) and 4(b) and Figs. 4(c) and 4(d), however, is not affected by the different topography of the surface where the film was deposited. This is consistent with the idea that the rates of kinetic processes are fixed by growth parameters—such as temperature and group III flow. Higher growth temperatures and smaller group III flows provide a faster coalescence of the islands on the surface, filling up the pits more efficiently. The results shown in Fig. 4, however, indicate that the spatial distribution of the islands formed during homoepitaxy depends strongly on the morphology of the surface where the film is deposited, even when the film thickness is of the order of thousands of monolayers.

The close relationship between the mounds observed here and the initial surface can also be observed in Fig. 5. Here we present the morphologies for films grown on nominal substrates with increasing thicknesses. The morphology for the thicker film [$t \sim 1.5$ μm, Fig. 5(d)] does not present mounds, corresponding to the picture of a typical two-dimensional layer-by-layer growth. The distribution of depth and distance between the deep valleys forming the mounds is shown in Fig. 6. We can notice that the depth distribution becomes narrower as thickness increases, corresponding to the process of filling up the pits. The average distance, however, is not much altered after the growth of a 50-nm-thick film and corresponds to the mean distance between the deeper pits on the initial surface. Figure 7 shows the rms roughness as a function of film thickness for films grown directly on the substrate using two different growth rates at 530 °C. Mound formation at the beginning of the growth corresponds to the initial fast increase of roughness while surface planarization through mound coalescence leads to the subsequent approximately roughness exponential decay—which is slightly faster for lower growth rates—as shown in Fig. 7.

It is important to notice that these samples were cooled down to room temperature after growth, before removal from the vacuum chamber and exposure to air. This cooling process can be interpreted as a short-time annealing of the grown film. Sudijono *et al.*[19] have shown that sample annealing can alter the overall morphology of a grown sample. It changes from a dynamical equilibrium surface during growth[20] to a morphology that recovers the information from the substrate—in terms of the original miscut—after annealing.

We believe that the results we show here are not affected

FIG. 6. Distribution of mean spacing between the deep valleys forming the mounds and depth of these valleys for GaAs films corresponding to Fig. 5: (a) 50 nm, (b) 150 nm, and (c) 300 nm. No mounds are observed for the 1500-nm-thick sample.

by this short-time annealing. The morphologies observed are very much dependent on growth parameters, indicating that the interplay between deposition and diffusion during growth determines the structures formed on the surface. Also, islands with small lateral dimensions can still be observed on top of the terraces after the sample cool down (Fig. 2). In this sense, we have also observed that mounds do not disappear with short-time annealing at growth temperature (for time periods corresponding to the sample cool down), even though microscopic roughness slightly decreases with this process.

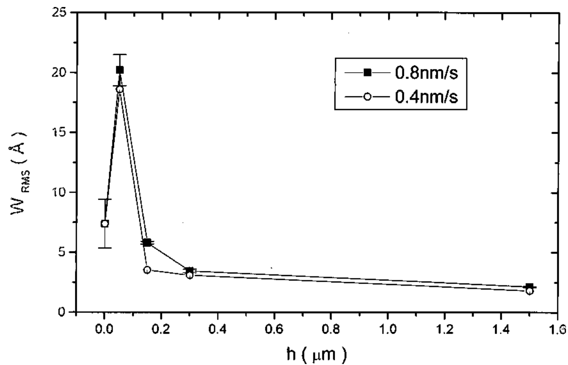

FIG. 7. rms roughness of GaAs films (for a 2×2-μm^2 area) as a function of film thickness for two different growth rates at 530 °C.

It is interesting to point out that no mound structures similar to those reported in the literature for GaAs grown on nominal surfaces by MBE (Refs. 7 and 15) were observed in our samples. In particular, we have used much higher growth rates than those generally considered by other authors, thus increasing the probability of a transition to a three-dimensional growth mode. In spite of this fact the transition was not observed, as it was in the case of homoepitaxial InP grown by CBE.[21,22] In that case, a transition from a smooth to a rougher, grainlike surface occurs for films grown under similar conditions of temperature and growth rate. For such rough InP surfaces, monolayer terraces are not resolved by

AFM. In our case, however, monolayer islands can be observed for GaAs films grown on nominal substrates for all conditions used in this work, indicating a stable layer-by-layer growth mode.

The idea that mound formation in our case is mainly related to the large break in symmetry of GaAs surfaces provided by the pits is also supported by theoretical calculations. Elkinani and Villain[23] have proposed a one-dimensional model (Zeno model) where healing of defects is observed for the case of no step edge barrier. When the presence of such a barrier is considered, the surface profile of a film starting from an initially flat surface presents cracks. In a more recent work, Politi and Villain[24] show that a mound structure arises during growth only after a time $t^* \approx 1/l_S$—where l_S is a parameter characterizing a step edge barrier, or Schwoebel effect[14]—and with a wavelength $\lambda_C \approx 1/\sqrt{l_S}$, allowing healing of surface defects with size smaller than λ_C during growth. Our results—showing the healing of pits from the initial GaAs surface through mound formation and coalescence, the similar results for both nominal and 2° off substrates and the absence of mounds for films grown on initially-flat surfaces as well as the absence of a growth mode transition—suggest a negligible ($l_S \rightarrow 0$) energy barrier at step edges for GaAs grown by CBE.

In summary, we observe mound formation in GaAs homoepitaxy. The presence of mounds is associated to a stage during the healing process of the initial GaAs surface. As film thickness increases, mounds coalesce and the surface evolves to that expected from a typical two-dimensional layer-by-layer growth mode, with wide terraces and few monolayer islands, independent of growth conditions. The monolayer island size distribution is determined by the kinetic conditions employed for the growth; the nucleation sites and island spatial distribution, however, are strongly influenced by the topography of the initial surface where the film is deposited, even for films thousands of monolayers thick. The healing of the initial surface, the similar morphologies observed for films grown on both nominal and 2° off substrates and the absence of mounds for films grown on initially flat surfaces indicate a negligible barrier for adatom movement across step edges in CBE-grown GaAs.

This work was financially supported by FAPESP, CNPq, and FINEP. One of the authors (V.R.C.) acknowledges financial support from CNPq.

[1] J. Villain, J. Phys. I **1**, 19 (1991).
[2] A. W. Hunt, C. Orme, D. R. M. Williams, B. G. Orr, and L. M. Sander, Europhys. Lett. **27**, 611 (1994).
[3] M. Siegert and M. Plischke, Phys. Rev. Lett. **68**, 2035 (1992).
[4] P. Smilauer and D. D. Vvedensky, Phys. Rev. B **52**, 14 263 (1995).
[5] G. W. Smith, A. J. Pidduck, C. R. Whitehouse, J. L. Glasper, A. M. Keir, and C. Pickering, Appl. Phys. Lett. **59**, 3282 (1991).
[6] G. W. Smith, A. J. Pidduck, C. R. Whitehouse, J. L. Glasper, and J. Spoward, J. Cryst. Growth **127**, 966 (1993).
[7] C. Orme, M. D. Johnson, J. L. Sudijono, K. T. Leung, and B. G. Orr, Appl. Phys. Lett. **64**, 860 (1994).
[8] J. E. Van Nostrand, S. J. Chey, D. G. Cahill, A. E. Botchkarev, and H. Morkoç, Surf. Sci. **346**, 136 (1996).
[9] H.-J. Ernst, F. Fabre, R. Folkerts, and J. Lapujoulade, Phys. Rev. Lett. **72**, 112 (1994).
[10] J.-K. Zuo and J. F. Wendelken, Phys. Rev. Lett. **78**, 2791 (1997).
[11] J. E. Van Nostrand, S. J. Chey, M.-A. Hasan, D. G. Cahill, and J. E. Greene, Phys. Rev. Lett. **74**, 1127 (1995).
[12] A. Stroscio, D. T. Pierce, M. D. Stiles, A. Zangwill, and L. M. Sander, Phys. Rev. Lett. **75**, 4246 (1995).
[13] G. Ehrlich and F. G. Hudda, J. Chem. Phys. **44**, 1039 (1966).
[14] R. L. Schwoebel and E. J. Shipsey, J. Appl. Phys. **37**, 3682 (1966).
[15] C. Orme, M. D. Johnson, K.-T. Leung, B. G. Orr, P. Smilauer, and D. Vvedensky, J. Cryst. Growth **150**, 128 (1995).
[16] M. Albrecht, H. Fritzsche, and U. Gradmann, Surf. Sci. **294**, 1 (1993).
[17] S. Morelhão and L. P. Cardoso, J. Appl. Crystallogr. **29**, 446 (1996).
[18] M. D. Johnson, C. Orme, A. W. Hunt, D. Graff, J. Sudijono, L. M. Sander, and B. G. Orr, Phys. Rev. Lett. **72**, 116 (1994).
[19] J. Sudijono, M. D. Johnson, M. B. Elowitz, C. W. Snyder, and B. G. Orr, Surf. Sci. **280**, 247 (1993).
[20] M. D. Johnson, J. Sudijono, A. W. Hunt, and B. G. Orr, Appl. Phys. Lett. **64**, 484 (1994).
[21] M. A. Cotta, R. A. Hamm, T. W. Staley, S. N. G. Chu, L. R. Harriott, M. B. Panish, and H. Temkin, Phys. Rev. Lett. **70**, 4106 (1993).
[22] M. A. Cotta, R. A. Hamm, S. N. G. Chu, L. R. Harriott, and H. Temkin, J. Appl. Phys. **75**, 630 (1994).
[23] I. Elkinani and J. Villain, J. Phys. I **4**, 949 (1994).
[24] P. Politi and J. Villain, Phys. Rev. B **54**, 5114 (1996).